Inorg. Chem. **2004**, *43*, 8561–8571

Inorganic Chemistry
Article

Structural Increment System for 11-Vertex *nido*-Boranes and Carboranes

Farooq A. Kiani[†,‡] **and Matthias Hofmann***[,†]

Anorganisch-Chemisches Institut, Ruprecht-Karls-Universität Heidelberg,
Im Neuenheimer Feld 270, D-69120 Heidelberg, Germany, and Department of Chemistry,
Quaid-I-Azam University, Islamabad, Pakistan

Received June 23, 2004

An increment system forming a set of quantitative rules that govern the relative stabilities of 11-vertex *nido*-boranes and carboranes is presented. Density functional theory computations at the B3LYP/6-311+G**//B3LYP/6-31G* level with ZPE corrections were carried out for 61 different boron hydride and carborane structures from $[B_{11}H_{14}]^-$ to $C_4B_7H_{11}$ to determine their relative stabilities. Disfavored structural features that destabilize a cluster structure relative to a hypothetical ideal situation were identified and weighted by so-called energy penalties. The latter show additive behavior and allow us to reproduce (within 5 kcal mol^{-1}) the DFT computed relative energies. Energy penalties for four structural features, i.e., adjacent carbon atoms, CC, a hydrogen atom bridging between a carbon and a boron atom, CH–B, an *endo*-terminal hydrogen atom at an open face carbon atom, CH_2 and an *endo*-H between two carbon atoms, $C(BH_2)C$ for the 11-vertex *nido*-cluster are quite similar to those reported for the 6-vertex *nido*-cluster, thus showing a behavior independent of the cluster size. Hydrogen structural features, however, vary strongly with the cluster size. Two unknown 11-vertex *nido*-carboranes were identified which are thermodynamically more stable than known positional isomers.

1. Introduction

Boranes played a major role in the development of a general concept of chemical bonds as their nonclassical structures cannot be described by single Lewis formula, but multicenter bonding needs to be considered. Since the discovery of the first carboranes in the 1960s,[1,2] carborane chemistry has gotten primary importance especially because of their typical structural patterns and bonding features. According to Wade's rule,[3] boranes and carboranes can be classified by their number of skeletal electrons (SE): *closo* ($2n + 2$ SE) with general formula $C_xB_{n-x}H_{n-x+2}$, *nido* ($2n + 4$ SE) with general formula $C_xB_{n-x}H_{n-x+4}$, and *arachno* ($2n + 6$ SE) with the general formula $C_xB_{n-x}H_{n-x+6}$. *closo*-Clusters adopt the shape of the most spherical deltahedra.[4] *nido*-Deltahedral fragments are obtained by the removal of one most highly coordinated vertex from *closo*-deltahedra. Further removal of a most highly coordinated vertex from the open face of a *nido*-deltahedral fragment gives an *arachno*-deltahedral fragment. According to empirical rules by Williams[5,6] for the placement of carbon atoms within a given carborane cluster, a carbon atom always tends to occupy the position of least connectivity in the thermodynamically most stable isomer. Furthermore, carbon atoms tend to occupy nonadjacent vertices if equivalently connected sites are available. Williams' carbon placement rules apply strictly to all *closo*-carboranes and even to other *closo*-heteroboranes and *closo*-heterocarboranes. But for *nido*-clusters, these rules are strictly followed only when there are no skeletal hydrogens at the open face. The placement of both skeletal bridge hydrogens and skeletal *endo*-hydrogens are of greater influence than the carbon location in the case of *nido*-deltahedral fragments.[7] The presence of

---

* To whom correspondence should be addressed. E-mail: matthias.hofmann@aci.uni-heidelberg.de.

[†] Ruprecht-Karls-Universität Heidelberg.

[‡] Quaid-I-Azam University.

(1) Grimes, R. N. *Carboranes*; Academic: New York, 1970. See references therein.

(2) Štíbr, B. *Chem. Rev.* **1992**, *92*, 225−250.

(3) (a) Wade, K. *Adv. Inorg. Chem. Radiochem.* **1976**, *18*, 1−66. (b) Wade, K. In *Metal Interactions with Boron Clusters*; Grimes, R. N., Ed.; Plenum Press: New York, 1982; Chapter 1, pp 1−41.

(4) (a) Williams, R. E. *Adv. Inorg. Chem. Radiochem.* **1976**, *18*, 67−142. (b) Williams, R. E. *Inorg. Chem.* **1971**, *10*, 210−214. (c) Williams, R. E. In *Borane, Carborane, Carbocation Continuum*; Casanova, J., Ed.; Wiley-Interscience: New York, 1998; Chapter 1, pp 3−57.

(5) Williams, R. E. *J. Am. Chem. Soc.* **1965**, *87*, 3513−3515.

(6) Williams, R. E. In *Progress in Boron Chemistry*; Brotherton, R. J., Steinberg, H., Eds.; Pergamon Press: England, 1970; Vol. 2, Chapter 2, p 57.

(7) Williams, R. E. *Chem. Rev.* **1992**, *92*, 177−207 and references therein.

10.1021/ic049184z CCC: $27.50

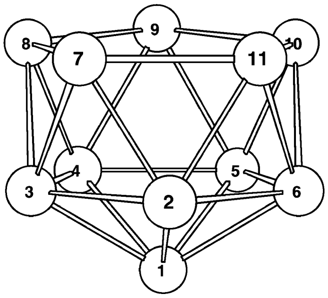

Figure 1. Numbering scheme for the 11-vertex *nido*-cluster.

the face hydrogen atoms makes necessary additional rules along with the two basic rules for a satisfactory explanation of different *nido*-boranes and carboranes. Such rules have already been reported for 73 structures of 6-vertex *nido*-boranes and carboranes from $[B_6H_9]^-$ to $C_4B_2H_6$,[8] using MP2(fc)/6-31G* level of theory.[9] In the present work, we explore the rules for the 11-vertex *nido*-cluster (shown in Figure 1) which can be considered as an extended 6-vertex *nido*-cluster with an additional five-membered ring between the open face and the apex.

In general, not all rules for an optimal arrangement of heteroatoms and *endo*-hydrogen atoms can be followed in all cases. Hence, a weighting scheme according to the importance of different rules is needed in order to decide violation of which rule (or rules) is best tolerated. We tried to establish such weights based on the assumptions that (1) deviation from a hypothetical ideal situation leads to destabilization of a cluster structure and (2) the amount of destabilization is additive. The disfavoring features that destabilize a cluster structure relative to the ideal situation are assigned increments also called energy penalties. More than one feature in a single cluster structure should result in a total destabilization equal to the sum of individual contributions. Provided the above assumptions are valid, an increment system assigning penalties to a few structural increments allows estimating the relative stabilities of isomeric clusters with satisfactory accuracy. We found excellent agreement between the computed relative energies (E_{B3LYP}'s) and those derived from our increment system (E_{inc_rel}'s).

Out of all *nido*-clusters, the 11-vertex *nido*-cluster has the maximum number of known examples for boranes and carboranes. For example, to the best of our knowledge, only 15 borane and carborane structure were known for the 6-vertex *nido*-cluster in 2001,[7] and 10 structures for 10-vertex *nido*-boranes and carboranes were known in 1992.[2,7] For the 11-vertex *nido*-boranes and carboranes, however, 29 structures or their alkyl derivatives/metal complexes are known from $[B_{11}H_{14}]^-$ to $C_4B_7H_{11}$. They have been included in this study and are listed in this paper (Tables 2 and 3).

2. Computational Details

Geometries were optimized at the density functional level employing the B3LYP hybrid functional together with the 6-31G(d) basis set using the *Gaussian 98* program.[10] Symmetry restrictions if applied are indicated in Table 2. All the structures except five (see Table 2) presented in this paper are local minima at B3LYP/6-31G(d) as determined by frequency calculations. Single point energies computed at B3LYP/6-311+G(d,p) together with zero point corrections at the B3LYP/6-31G(d) level were used to derive relative energies. These computed relative energies are to be reproduced by an energy increment system. Certain geometrical features were identified and assigned reasonable preliminary energy penalties by comparison of suitable isomeric clusters. The values were refined through a statistical fitting procedure. Final values recommended for use were in part slightly modified in order to better reproduce the stability order which results from DFT computations. Values arising from the fitting procedure as well as the modified values are given in Table 1. The aim was to reproduce the computed relative energies well (i.e., with a 5 kcal mol^{-1} accuracy) with as few penalties as possible.

3. Result and Discussion

An increment system has been devised from a total of 61 anionic or neutral (car)borane structures from $[B_{11}H_{14}]^-$ to $C_4B_7H_{11}$. Nine quantitative rules suffice to correctly describe the relative stabilities of all these boranes and carboranes. Out of the 61 isomers considered here, 29 structures or their alkyl derivatives/metal complexes (Table 3) have so far been characterized experimentally. Some of the unknown structures may never be known but are still of interest to explore the principles governing the thermodynamic stabilities. In Table 2, the label "a" marks known isomers. The synthesis of some unknown isomers should be possible as they are thermodynamically more stable as compared to experimentally known isomers. These isomers are labeled "b" in Table 2.

3.1. Selection of Structural Features. Initially, those structural features reported for 6-vertex *nido*-boranes and carboranes[8] were considered for the 11-vertex *nido*-boranes and carboranes. Some of the structural features are identical in the 6- and 11-vertex case: (a) CC, a structural feature for two adjacent carbon atoms, (b) BH_2, a feature that involves an *endo*-terminal hydrogen atom attached to an open face boron atom, (c) CH_2, where an *endo*-terminal hydrogen atom is attached to an open face carbon atom, (d) $C(BH_2)C$, where a BH_2 group is located between two carbon atoms, and (e) CH−B, which symbolizes a CB bridging hydrogen atom closer to the carbon atom.

---

(8) Hofmann, M.; Fox, M. A.; Greatrex, R.; Schleyer, P. v. R.; Williams, R. E. *Inorg. Chem.* **2001**, *40*, 1790−1801.

(9) According to our experience, B3LYP (used here) gives very similar results for carboranes as compared to MP2 (used in ref 8) but at less computational cost.

(10) Frisch, M. J.; Trucks, G. W.; Schlegel, H. B.; Scuseria, G. E.; Robb, M. A.; Cheeseman, J. R.; Zakrzewski, V. G.; Montgomery, J. A., Jr.; Stratmann, R. E.; Burant, J. C.; Dapprich, S.; Millam, J. M.; Daniels, A. D.; Kudin, K. N.; Strain, M. C.; Farkas, O.; Tomasi, J.; Barone, V.; Cossi, M.; Cammi, R.; Mennucci, B.; Pomelli, C.; Adamo, C.; Clifford, S.; Ochterski, J.; Petersson, G. A.; Ayala, P. Y.; Cui, Q.; Morokuma, K.; Malick, D. K.; Rabuck, A. D.; Raghavachari, K.; Foresman, J. B.; Cioslowski, J.; Ortiz, J. V.; Stefanov, B. B.; Liu, G.; Liashenko, A.; Piskorz, P.; Komaromi, I.; Gomperts, R.; Martin, R. L.; Fox, D. J.; Keith, T.; Al-Laham, M. A.; Peng, C. Y.; Nanayakkara, A.; Gonzalez, C.; Challacombe, M.; Gill, P. M. W.; Johnson, B. G.; Chen, W.; Wong, M. W.; Andres, J. L.; Head-Gordon, M.; Replogle, E. S.; Pople, J. A. *Gaussian 98*, revision A.6; Gaussian, Inc.: Pittsburgh, PA, 1998.

Table 1. Structural Features and Energy Penalties for the 11-Vertex *nido*-Boranes and Carboranes Compared to the Corresponding Values for the 6-Vertex *nido*-Boranes and Carboranes

		energy penalty [kcal mol^{-1}]		
		11-vertex *nido*		
feature	symbol	value from the fitting procedure	modified value	6-vertex *nido*[a]
BHB adjacent[b]	HH	25.0	25.9	7
endo-BH between two BHB[b]	H(*endo*-H)H	22.2	23.9	*e*
endo-BH[b]	BH_2	2.3	2.1	11
5k carbon atom[c]	$C_{4k\to5k}$	28.0	28.0	*f*
carbon atoms adjacent[c]	CC	16.0	16.0	15
endo-hydrogen on carbon atom[d]	CH_2	33.2	33.2	30
hydrogen bridge between carbon and boron atoms[d]	CH−B	33.1	33.1	27
endo-BH between two carbon atoms[d]	$C(BH_2)C$	28.8	28.8	25
carbon next to BHB[d]	C(H)	2.2	2.2	*g*

[a] In this table, only those energy penalties for the 6-vertex *nido*-cluster which are comparable to the 11-vertex *nido*-cluster are listed. For all energy penalties, see ref 8. All structures were computed at MP2(fc)/6-31G(d). [b] Hydrogen structural features. [c] Carbon structural features. [d] Mixed structural features. [e] Structural feature covered differently for 6-vertex *nido*-boranes and carboranes.[8] [f] The energy penalty $C_{3k\to5k}$ for the 6-vertex *nido*-cluster for a carbon atom at a 5k instead of a 3k vertex is 33 kcal mol^{-1}. [g] The feature C(H) has no significance for the 6-vertex *nido*-cluster as all the possibilities have one carbon atom adjacent to a hydrogen bridge except one, i.e., 2-$CB_5H_7^{2-}$ (μ-H: 4/5).

Three features are new: What is called C_{5k} (carbon atom at a 5-coordinated vertex) in ref 8 more exactly is $C_{3k\to5k}$ (C at 5k instead of 3k vertex) for the 6-vertex *nido*-cluster, but $C_{4k\to5k}$ (C at 5k instead of 4k vertex) is needed for the 11-vertex *nido*-clusters. The favorable position for a carbon atom in both the 6- and 11-vertex *nido*-carboranes is a vertex of the open face due to lower connectivity. But in the 6-vertex *nido*-cluster, the open face vertices are threefold connected to other cluster atoms (3k) whereas in the 11-vertex *nido*-cluster, the open face vertices are 4k. The 6- and 11-vertex *nido*-clusters contain one and six 5k vertices, respectively, which are unfavorable for carbon atom placement. When a carbon atom is forced to occupy a 5k position, it needs to be referred to as $C_{3k\to5k}$ for the 6-vertex *nido*-cluster and $C_{4k\to5k}$ (see Figure 2b) for the 11-vertex *nido*-cluster.

The other two new structural features identified for the 11-vertex *nido*-boranes and carboranes, i.e., H(*endo*-H)H and C(H) are illustrated in Figure 2a,c and are explained in sections 3.2.1 and 3.2.3, respectively.

Two types of hydrogen adjacent energy penalties were described for the 6-vertex *nido*-cluster designated as HA-0 and HA-1 (where the extra number refers to the number of *endo*-BH 2c−2e bonds).[8] For the 11-vertex *nido*-cluster, only one energy penalty (i.e., HH Figure 2a) suffices. Table 1 lists the nine structural features for the 11-vertex *nido*-cluster with corresponding increments. Values for comparable structural features for the 6-vertex *nido*-cluster are also given.

Some features found for the 6-vertex *nido*-cluster[8] were not present in any of the optimized 11-vertex *nido*-borane and carborane geometries: (a) C−HB, where a bridging hydrogen atom is closer to a boron atom than to a carbon atom and its related C(CHB) feature, (b) 5k(HA_0) and 5k-(HA_1), where a 5k carbon atom is in the vicinity of two adjacent hydrogen bridges, and (c) additional structural features related to CH_2 and CHB (CH_2 and CHB are already high energy features). That is, $C(CH_2)$, $C(CH_2)C$, and C(CHB) result in further increase in energy of the cluster[8] and are not included in this study of the 11-vertex *nido*-cluster.[11] It is highly unlikely that any 11-vertex *nido*-cluster containing these features would have competitive thermodynamic stability. Section 3.5 and Table 1 give a detailed comparison of carbon, hydrogen, and mixed structural features for the 6- and 11-vertex *nido*-clusters.

3.2. Energy Penalties for the 11-Vertex *nido*-Boranes and Carboranes. The final nine structural increments for borane and carborane isomers from $[B_{11}H_{14}]^-$ to $C_4B_7H_{11}$ derived in this work are listed in Table 1 and are also illustrated in Figure 2.

The different structural features related to *endo*-hydrogen placement (see Figure 2a) are defined in the next section; those that are due to carbon atom placement (see Figure 2b) follow in section 3.2.2. Mixed features which involve both carbon and hydrogen atoms are described in section 3.2.3 (see Figure 2c).

3.2.1. Hydrogen Structural Features. HH. Two bridging hydrogen atoms adjacent to each other have an energy penalty of 25.9 kcal mol^{-1}.

H(*endo*-H)H. An *endo*-hydrogen between two hydrogen bridges involves an energy penalty of 23.9 kcal mol^{-1}.

BH_2. An *endo*-terminal hydrogen atom has an energy penalty of 2.1 kcal mol^{-1}.

3.2.2. Carbon Structural Features. $C_{4k\to5k}$. A carbon atom located at a 5k rather than a 4k position reduces the cluster stability by 28.0 kcal mol^{-1}. Among the 5k positions, positions 2−6 are slightly preferred over the apical position 1 (see Figure 1).

CC. Two carbon atoms adjacent to each other destabilize a structure by 16.0 kcal mol^{-1}. This is almost exactly the energy difference that is computed between the 1,2- and 1,7-

---

(11) Estimated energy penalties for $C(CH_2)$, $C(CH_2)C$, and C(CHB) are 11.6, 20.4, and 7.3 kcal mol^{-1} for the 11-vertex *nido*-cluster. These values are quite similar to 10, 17, and 5 kcal mol^{-1} for the corresponding structural features in the 6-vertex *nido*-cluster. The energy penalty for $C(CH_2)C$ can be considered as the double of $C(CH_2)$ in both 6- and 11-vertex *nido*-clusters. These penalties are only roughly estimated values as only one geometry was computed to derive the energy penalties for each of these features. The energy penalty $C(BH_2)$ (4.6 kcal mol^{-1}) in 11-vertex *nido*-cluster is also very close to that of $C(BH_2)$ (7 kcal mol^{-1}) in 6-vertex *nido*-cluster.

Table 2. Detailed Information on the 61 Isomers from $[B_{11}H_{14}]^-$ to $C_4B_7H_{11}$ Considered in This Study

	compd	extra hydrogen atoms	sym	HH 25.9	H(*endo*-H)H 23.9	BH_2 2.1	$C_{4k\rightarrow 5k}$ 28.0	CC 16.0	CH_2 33.2	CHB 33.1	$C(BH_2)C$ 28.8	C(H) 2.2	E_{inc_sum}	E_{inc_rel}	E_{B3LYP}	E_{diff}
AA[a]	$B_{11}H_{14}^-$	μ-H: 7/8, 9/10, 7/11	C_1	1									25.9	0.0	0.0	0.0
AB[b]	$B_{11}H_{14}^-$	μ-H:8/9, 10/11, *endo*-H: 7	C_1		1	1							26.0	0.1	0.2	0.1
BA[b]	$B_{11}H_{13}^{2-}$	μ-H: 7/8, 9/10	C_1										0.0	0.0	0.0	0.0
BB	$B_{11}H_{13}^{2-}$ (TS)	μ-H: 9/10, *endo*-H: 7	C_s			1							2.1	2.1	2.7	0.6
CA[b]	$B_{11}H_{12}^{3-}$	μ-H: 7/8	C_1										0.0	0.0	0.0	0.0
CB	$B_{11}H_{12}^{3-}$ (TS)	*endo*-H: 7	C_s			1							2.1	2.1	4.9	2.8
DA	1-$CB_{10}H_{14}$	μ-H: 8/9, 10/11, *endo*-H: 7	C_1		1	1	1						54.0	0.0	0.0	0.0
DB	2-$CB_{10}H_{14}$	μ-H: 8/9, 9/10, 7/11	C_1	1			1					1	56.1	2.1	1.4	−0.7
DC	7-$CB_{10}H_{14}$	μ-H: 8/9, 9/10, 10/11	C_1	2								2	56.2	2.2	3.2	1.0
DD	7-$CB_{10}H_{14}$	μ-H: 8/9, 9/10, *endo*-H: 7	C_1		1				1			2	61.5	7.5	6.6	−0.9
DE	2-$CB_{10}H_{14}$	μ-H: 7/8, 10/11, *endo*-H: 9	C_1		1	1	1					2	58.4	4.4	7.4	3.0
EA[b]	7-$CB_{10}H_{13}^-$	μ-H: 8/9, 10/11	C_1									2	4.4	0.0	0.0	0.0
EB[b]	1-$CB_{10}H_{13}^-$	μ-H: 7/8, 9/10	C_s				1						28.0	23.6	23.0	−0.6
EC	2-$CB_{10}H_{13}^-$	μ-H: 8/9, 7/11	C_1				1					1	30.2	25.8	23.4	−2.4
ED	7-$CB_{10}H_{13}^-$ (TS)	μ-H: 9/10, *endo*-H: 7	C_s						1				33.2	28.8	29.2	0.4
FA	7-$CB_{10}H_{12}^{2-}$	μ-H: 9/10	C_1										0.0	0.0	0.0	0.0
FB	7-$CB_{10}H_{12}^{2-}$	μ-H: 8/9	C_1									1	2.2	2.2	1.8	−0.4
FC	2-$CB_{10}H_{12}^{2-}$	μ-H: 8/9	C_1				1						28.0	28.1	24.6	−3.4
FD	2-$CB_{10}H_{12}^{2-}$ (TS)	*endo*-H: 9	C_s			1	1						30.1	30.1	27.2	−2.9
FE	2-$CB_{10}H_{12}^{2-}$	μ-H: 7/11	C_1				1					1	30.2	30.2	28.9	−1.3
FF	2-$CB_{10}H_{12}^{2-}$	μ-H: 7/8	C_1				1					1	30.2	30.2	29.8	−0.4
GA[b]	7-$CB_{10}H_{11}^{3-}$		C_s										0.0	0.0	0.0	0.0
GB	2-$CB_{10}H_{11}^{3-}$		C_s				1						28.0	28.0	26.0	−2.0
GC	1-$CB_{10}H_{11}^{3-}$		C_{5v}				1						28.0	28.0	28.8	0.8
HA[c]	2,8-$C_2B_9H_{13}$	μ-H: 9/10, 7/11	C_1				1					3	34.6	0.0	0.0	0.0
HB[d]	1,7-$C_2B_9H_{13}$	μ-H: 8/9, 10/11	C_1				1					2	32.4	−2.2	0.6	2.8
HC[b]	2,9-$C_2B_9H_{13}$	μ-H: 7/8, 10/11	C_1				1					4	36.8	2.2	5.8	3.6
HD[b]	7,8-$C_2B_9H_{13}$	μ-H: 9/10, 10/11	C_s	1				1				2	46.3	11.7	9.7	−2.0
HE[c]	2,7-$C_2B_9H_{13}$	μ-H: 8/9, 10/11	C_1				1	1				3	50.6	16.0	15.1	−0.9
HF[e]	1,7-$C_2B_9H_{13}$ (TS)	μ-H: 9/10, *endo*-H: 7	C_s				1		1				61.2	26.6	28.8	2.2
HG	7,9-$C_2B_9H_{13}$	μ-H: 9/10, 7/11	C_s							2			66.2	31.6	30.2	−1.4
HH[e]	1,7-$C_2B_9H_{13}$	μ-H: 8/9, 7/11	C_1				1			1		1	63.3	28.7	31.2	2.5
HI	1,2-$C_2B_9H_{13}$	μ-H: 7/8, 9/10	C_1				2	1				1	74.2	39.6	40.2	0.6
HJ	1,2-$C_2B_9H_{13}$	μ-H: 7/8, 10/11	C_s				2	1				2	76.4	41.8	46.7	4.9
IA[b]	7,9-$C_2B_9H_{12}^-$	μ-H: 10/11	C_1									2	4.4	0.0	0.0	0.0
IB[b]	7,8-$C_2B_9H_{12}^-$	μ-H: 9/10	C_1					1				1	18.2	13.8	15.7	1.9
IC[b]	7,8-$C_2B_9H_{12}^-$	*endo*-H: 10	C_s			1		1					18.0	13.6	15.9	2.3
ID[b]	2,9-$C_2B_9H_{12}^-$	μ-H: 7/11	C_1				1					1	30.2	25.8	25.9	0.1
IE[e,f]	7,9-$C_2B_9H_{12}^-$	*endo*-H: 8	C_1			1					1		30.9	26.5	27.0	0.5
IF[c]	2,8-$C_2B_9H_{12}^-$	μ-H: 7/11	C_1				1					2	32.4	28.0	29.1	1.1
IG[c]	2,7- $C_2B_9H_{12}^-$	μ-H: 9/10	C_1				1	1					44.0	39.6	36.9	−2.7
IH	2,4-$C_2B_9H_{12}^-$	μ-H: 8/9	C_1				2					1	58.2	53.8	53.5	−0.3
II	1,7-$C_2B_9H_{12}^-$	*endo*-H: 7	C_s				1		1				61.2	56.8	57.4	0.6
IJ	1,2-$C_2B_9H_{12}^-$	μ-H: 8/9	C_1				2	1					72.0	67.6	67.4	−0.2
IK	2,3-$C_2B_9H_{12}^-$	μ-H: 8/9	C_1				2	1				1	74.2	69.8	69.3	−0.5
IL	1,2-$C_2B_9H_{12}^-$	μ-H: 7/11	C_1				2	1				2	76.4	72.0	71.9	−0.1
JA[b]	7,9-$C_2B_9H_{11}^{2-}$		C_s										0.0	0.0	0.0	0.0
JB[b]	7,8-$C_2B_9H_{11}^{2-}$		C_s					1					16.0	16.0	16.3	0.3
JC[b]	2,9-$C_2B_9H_{11}^{2-}$		C_s				1						28.0	28.0	27.1	−0.9
JD[g]	2,8-$C_2B_9H_{11}^{2-}$		C_1				1						28.0	28.0	29.1	1.1
JE[g]	1,7-$C_2B_9H_{11}^{2-}$		C_s				1						28.0	28.0	33.0	5.0
JF[g]	2,7-$C_2B_9H_{11}^{2-}$		C_1				1	1					44.0	44.0	42.5	−1.5
JG[g]	2,4-$C_2B_9H_{11}^{2-}$		C_1				2						56.0	56.0	57.4	1.4
JH	1,2-$C_2B_9H_{11}^{2-}$		C_1				2	1					72.0	72.0	74.6	2.6
KA[b]	7,8,9-$C_3B_8H_{12}$	μ-H: 10/11	C_1					2				2	36.4	0.0	0.0	0.0
KB	7,8,10-$C_3B_8H_{12}$	*endo*-H: 9	C_1			1		1			1		46.9	10.5	11.7	1.2
LA[b]	7,8,10-$C_3B_8H_{11}^-$		C_1					1					16.0	0.0	0.0	0.0
LB[b]	7,8,9-$C_3B_8H_{11}^-$		C_1					2					32.0	16.0	18.5	2.5
MA[b]	7,8,9,10-$C_4B_7H_{11}$		C_1					3					48.0	0.0	0.0	0.0
MB[b]	1,7,8,10-$C_4B_7H_{11}$		C_1				1	1					44.0	−4.0	0.7	4.7
MC[b]	2,7,9,10-$C_4B_7H_{11}$		C_1				1	2					60.0	12.0	8.3	−3.7

[a] For **AA**, only 7-X-derivatives are known (where X = OH, OEt, Py, etc.). [b] Experimentally known structures. [c] Only methyl derivatives are experimentally known. [d] Strong candidates. [e] **HH** and **HF** differ from **HB** only in the position of *endo*-hydrogen atoms. [f] **IE** differs from **IA** only in the position of the *endo*-hydrogen atom. All the structures are minima except where TS indicates a transition state. [g] Only metal complexes are experimentally known.

Table 3. Experimentally Known 11-Vertex *nido*-Carboranes

compd	extra hydrogen atoms	reference[a]				
		synthesis	X-ray	NMR	ab initio/DFT	reviewed
7-X-$B_{11}H_{13}^-$ (7-X derivative of **AA**)	μ-H: 7/8, 9/10, 7/11	32 (X= OH, OEt, Py),	32 (X= OEt, Py)	32 (X= OH, OEt, Py)	32 (X= OH, OEt, Py)	
$B_{11}H_{14}^-$ (**AB**)	μ-H: 8/9, 10/11, *endo*-H: 7	33, 34	35, 36	33	37	7, 38
$B_{11}H_{13}^{2-}$ (**BA**)	μ-H: 7/8, 9/10	39, 19	40	19		7, 38
$B_{11}H_{12}^{3-}$ (**CA**)	μ-H: 7/8	19		19	19, 41	38
7-$CB_{10}H_{13}^-$ (**EA**)	μ-H: 8/9, 10/11	22	42		22	1, 20, 21
1-$CB_{10}H_{13}^-$ (**EB**)	μ-H: 7/8, 9/10	23		23		
7-$CB_{10}H_{11}^{3-}$ (**GA**) and metal complexes		12, 13, 14	12, 13, 14	12, 13, 14	13	
methyl derivatives of 2,8-$C_2B_9H_{13}$ (**HA**)	μ-H: 9/10, 7/11	18		18	18	
2,9-$C_2B_9H_{13}$ (**HC**)	μ-H: 7/8, 10/11	43, 24, 44[b]		24	24, 44	2
7,8-$C_2B_9H_{13}$ (**HD**)	μ-H: 9/10, 10/11	25a, 24		24	24, 44	2
methyl derivatives of 2,7-$C_2B_9H_{13}$ (**HE**)	μ-H: 8/9, 10/11	17, 18	17	17, 18	17, 18	2
7,9-$C_2B_9H_{12}^-$ (**IA**)	μ-H: 10/11	25b, 24	24	25b, 24	24	2, 7
7,8-$C_2B_9H_{12}^-$ (**IB**)	μ-H: 9/10	25, 26,[c] 24, 27[d]	45, 27	25b, 24, 27	24	2, 7
7,8-$C_2B_9H_{12}^-$ (**IC**)	*endo*-H: 10	26,[c] 46	46	46		
2,9-$C_2B_9H_{12}^-$ (**ID**)	μ-H: 7/11	47, 24	24	47, 24	24	
alkyl derivatives of 2,7-$C_2B_9H_{12}^-$ (**IG**)	μ-H: 9/10	48, 18		18	18	
7,9-$C_2B_9H_{11}^{2-}$ (**JA**) and metal complexes		49, 50, 51, 15	49[e]	49, 15	15	7
7,8-$C_2B_9H_{11}^{2-}$ (**JB**) and metal complexes		52, 49, 51, 15	52[f]	49, 15	15	7
2,9-$C_2B_9H_{11}^{2-}$ (**JC**)		47, 15		47, 15	15	
cyclopetadienyl cobalt complexes of 2,8- (**JD**), 1,7- (**JE**), 2,7- (**JF**), and 2,4-$C_2B_9H_{11}^{2-}$ (**JG**)		53		53		
7,8,9-$C_3B_8H_{12}$ (**KA**)	μ-H: 10/11	28		28	28	
7,8,10-$C_3B_8H_{11}^-$ (**LA**)		28		28	28	
7,8,9-$C_3B_8H_{11}^-$ (**LB**)		28		28	28	
7,8,9,10-$C_4B_7H_{11}$ (**MA**)		29		29	30	2, 7
1,7,8,10-$C_4B_7H_{11}$ (**MB**)		31		31	30	7
2,7,9,10-$C_4B_7H_{11}$ (**MC**)		29		29	30	7

[a] In the case of more than one reference, the compound was first reported in the first reference; for example, synthesis of $B_{11}H_{13}^{2-}$ (**BA**) was first reported in 1988 (ref 39) and again in 2001 (ref 19). [b] Molecular structure determination by gas-phase electron diffraction. [c] Raman spectra were reported in ref 26. [d] Molecular structure determination by neutron diffraction. [e] First single-crystal X-ray characterization of metal complexes of 7,8-$C_2B_9H_{11}^{2-}$ to the best of our knowledge. [f] First single-crystal X-ray characterization of metal complexes of 7,9-$C_2B_9H_{11}^{2-}$ to the best of our knowledge.

isomers of *closo*-$C_2B_{10}H_{12}$ (15.9 kcal mol^{-1} in favor of the latter, i.e., meta carborane). A *para*-arrangement of carbon atoms is slightly preferred over a *meta*-arrangement in both *closo*-dicarboranes (1,12- is more stable than 1,7-$C_2B_{10}H_{12}$ by 2.3 kcal mol^{-1}) and *nido*-dicarboranes (2,9- is more stable than $[2,8\text{-}C_2B_9H_{11}]^{2-}$ by 2.0 kcal mol^{-1}). An *ortho*-relationship is much more destabilizing than a *meta*-relationship of carbon atoms. However, we do not differentiate *meta*- and *para*-arrangements here, as it turned out that considering only CC (*ortho*-carbon atoms) works well and this keeps the scheme simple.

3.2.3. Mixed Structural Features. Features that involve carbon, hydrogen, and/or boron atoms include the following.

CH_2. An *endo*-terminal hydrogen atom attached to an open-face carbon atom has an energy penalty of 33.2 kcal mol^{-1}.

CH−B. A hydrogen atom bridging a carbon and a boron atom results in an increase in energy of the respective structure by 33.1 kcal mol^{-1}.

C(BH_2)C. An *endo*-terminal hydrogen between two carbon vertices owes an energy penalty of 28.8 kcal mol^{-1}.

C(H). A carbon atom adjacent to a bridging hydrogen atom increases the energy of a structure by 2.2 kcal mol^{-1}.

We note that extra hydrogen and carbon atoms closer to each other on the open face result in higher energy penalties (Scheme 1). Structures with a 4k carbon atom separated from a H-bridge or a BH_2 group have energy penalties of 0 and 2.1 kcal mol^{-1}, respectively. The H-bridge or BH_2 group next to a carbon atom has 2.2 and 4.6 kcal mol^{-1}, respectively.[11] Most destabilizing are the features with the extra H directly attached to the carbon atom, i.e., CHB and CH_2 (33.1 and 33.2 kcal mol^{-1}).

The closer the open face hydrogen atom is to the carbon atom, the greater the disfavoring effect of the corresponding structural feature.

3.3. 5k Splitting. The energy penalty, $C_{4k\rightarrow 5k}$, for locating a carbon atom at any of the 5k cage vertices rather than at a peripheral 4k vertex is 28.0 kcal mol^{-1}. However, it was found that, for the two isomers having the same structural features but differing in the positions of the 5k carbon atom, a carbon atom at positions 2−6 (see Figure 1) is more favorable as compared to a carbon atom at position number 1 for the 11-vertex *nido*-cluster (e.g., compare E_{B3LYP} for isomers **GB** and **GC**, or **JC** and **JD**, Table 2). In an attempt to determine the separate energy penalties for positions 1 and 2−6 for carboranes, the energy difference came out to be only 0.6 kcal mol^{-1}. In order to keep the overall increment scheme simple, this energy penalty is considered as a fine-tuning only which may be applied for differentiating isomers which are otherwise identical.

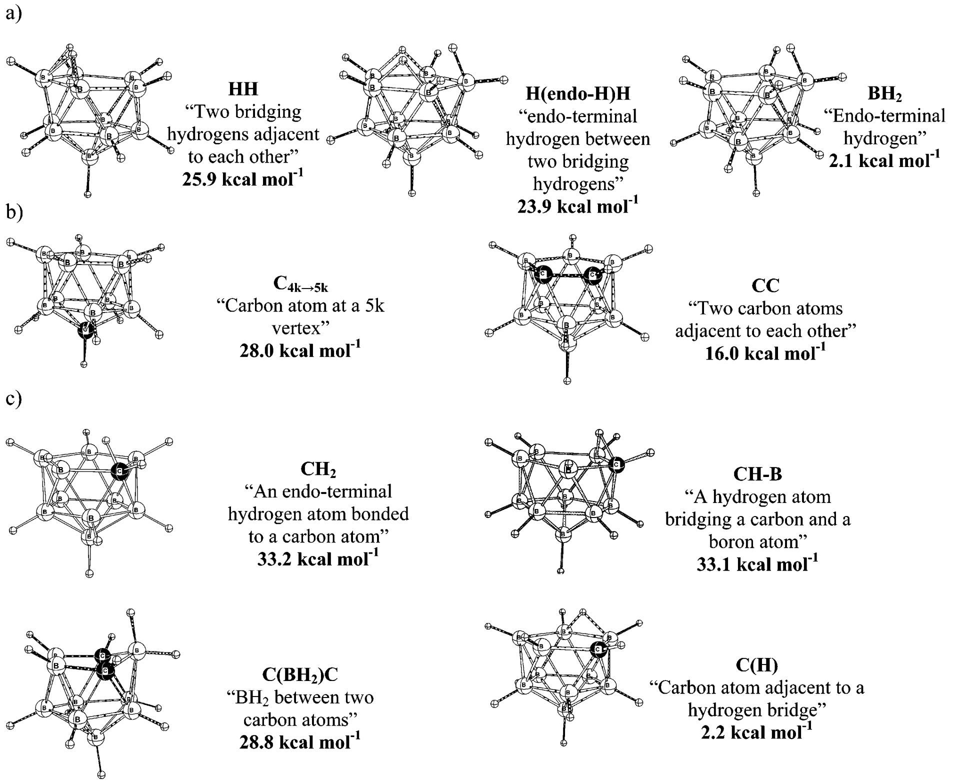

Figure 2. Structural features and corresponding energy penalties for the 11-vertex *nido*-carboranes family: (a) hydrogen, (b) carbon, and (c) mixed structural features.

Scheme 1. The Closer the Extra Hydrogen Atom Is to the Carbon Atom, the Higher the Energy Penalty for the Corresponding Structural Feature[a]

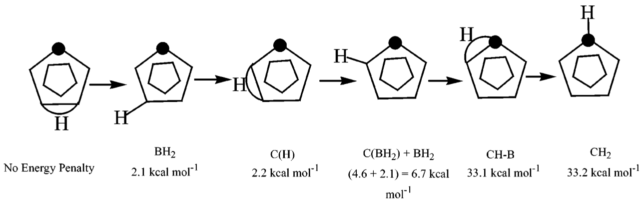

[a] See Table 1 and ref 10.

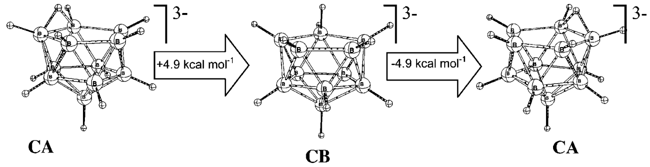

Figure 3. $[B_{11}H_{12}]^{3-}$ structures: **CB** represents the transition state for the hydrogen atom migration on the open face in minimum **CA**.

3.4. Why Do Carbon Atoms Occupy the Vertices of Larger Connectivity in Some Known Isomers? Carbon atoms occupy the open face positions in many known *nido*-carboranes. Examples for the 11-vertex *nido*-clusters are *nido*-7-$[CB_{10}H_{11}]^{3-}$ (**GA**)[12−14] and also *nido*-7,9-$[C_2B_9H_{11}]^{2-}$ (**JA**) studied recently by M. A. Fox et al.[15] Both **GA** and **JA** do not contain any skeletal hydrogen atoms, and qualitative rules already allow us to correctly identify the most stable isomer. But the case is not so simple always. Carbon atoms occupy cage vertices in the presence of skeletal hydrogens in some known *nido*-carboranes.[7] Examples are *nido*-1,2-$C_2B_3H_7$[7,16] and *nido*-7-Me-2,8-$C_2B_9H_{12}$.[7,17,18] With the help of separate quantitative rules for hydrogen and carbon placement patterns, it is possible to predict the relative energy of different *nido*-isomers with good accuracy. For instance, the presence of three extra hydrogens in the experimentally unknown *nido*-$CB_{10}H_{14}$ disfavors the open face positions for carbon placement in the most stable isomer. Therefore, the carbon atom occupies the apical 5k position in the thermodynamically most stable isomer **DA**, i.e., *nido*-1-$CB_{10}H_{14}$ (Figures 4, 5). Other isomers (Figure 4) with a carbon atom at position number 2, i.e., *nido*-2-$CB_{10}H_{14}$, **DB**, or position number 7, i.e., *nido*-7-$CB_{10}H_{14}$, **DC**, are higher in energy (by 1.4 and 3.2 kcal mol^{-1}, respectively). Similarly, in the case of *nido*-$C_2B_9H_{13}$, due to extra hydrogen atoms at the open face, the carbon atoms occupy vertices of larger connectivity in the thermodynamically most stable isomer *nido*-2,8-$C_2B_9H_{13}$, **HA**.

---

(12) Batten, S. A.; Jeffery, J. C.; Jones, P. L.; Mullica, D. F.; Rudd, M. D.; Sappenfield, E. L.; Stone, F. G. A.; Wolf A. *Inorg. Chem.* **1997**, *36*, 2570−2577.

(13) Blandford, I.; Jeffery, J. C.; Jelliss, P. A.; Stone, F. G. A. *Organometallics* **1998**, *17*, 1402−1411.

(14) Ellis, D.; Franken, A.; Jelliss, P. A.; Stone, F. G. A.; Yu P.-Y. *Organometallics* **2000**, *19*, 1993−2001.

(15) Fox, M. A.; Goeta, A. E.; Hughes A. K.; Johnson, A. L. *J. Chem. Soc., Dalton Trans.* **2002**, *9*, 2009−2019.

(16) Fox, M. A.; Greatrex, R.; Nikrahi, A.; Brain, P. T.; Picton, M. J.; Rankin, D. W. H.; Robertson, H. E.; Bühl, M.; Li, L.; Beaudet, R. A. *Inorg. Chem.* **1998**, *37*, 2166−2176.

(17) Struchkov, Yu. T.; Antipin, M. Yu.; Stanko, V. I.; Brattsev, V. A.; Kirillova, N. I.; Knyazev, S. P. *J. Organomet. Chem.* **1977**, *141*, 133−139.

(18) Fox, M. A.; Hughes, A. K.; Malget, J. M. *J. Chem. Soc., Dalton Trans.* **2002**, *18*, 3505−3517.

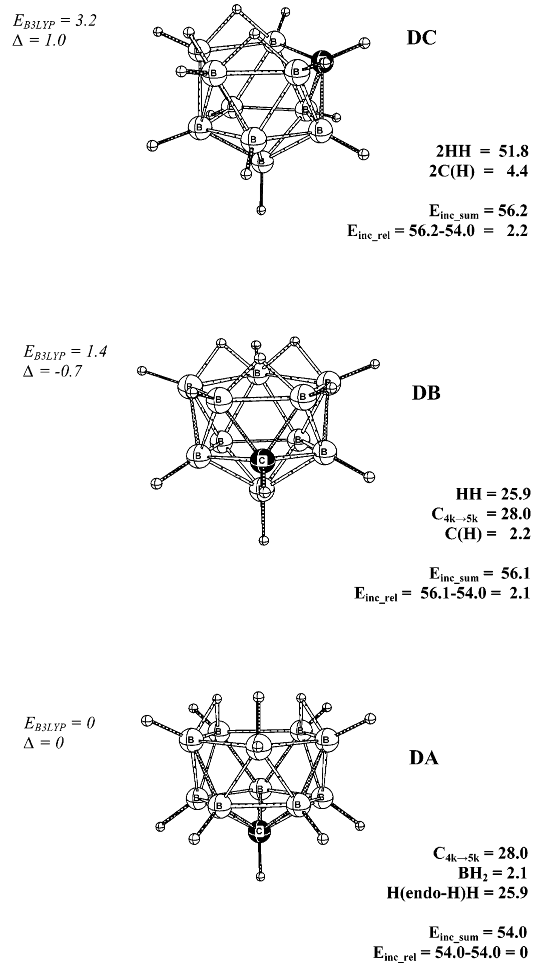

Figure 4. Use of the increment system exemplified for various isomers of $CB_{10}H_{14}$ from **DA** to **DC**.

3.5. A Comparison of Energy Penalties for the 11-Vertex and the 6-Vertex *nido*-Clusters. 3.5.1. Carbon Energy Penalties Are Independent of the Cluster Type. The CC structural feature (see Table 1) has quite similar energy penalties, i.e., 15 and 16.0 kcal mol^{-1} in the 6-vertex[8] and the 11-vertex *nido*-clusters, respectively, and hence seems to be independent of the cluster size. The $C_{4k\rightarrow 5k}$ feature of the 11-vertex *nido*-cluster is not present in the 6-vertex *nido*-cluster where $C_{3k\rightarrow 5k}$ applies instead. If $C_{3k\rightarrow 5k}$ and $C_{4k\rightarrow 5k}$ are independent of the cluster size, a value of 5 kcal mol^{-1} is expected for $C_{3k\rightarrow 4k}$. To estimate the latter increment more directly, two 10-vertex *nido*-$[CB_9H_{12}]^-$ isomers differing only in the position of carbon atoms were computed using B3LYP/6-311+G(d,p)//B3LYP/6-31G(d). The isomer with the carbon atom at position number 6 (3k) was 6.6 kcal mol^{-1} more stable than the isomer with the carbon atom at position number 5 (4k), being in good agreement with the above estimation.

3.5.2. Hydrogen Energy Penalties Vary with the Cluster Type. While carbon energy penalties for the 11-vertex *nido*-cluster are quite similar to those of the 6-vertex *nido*-cluster,[8] there is a huge difference for the hydrogen energy penalties between the two clusters (see Table 1).

Two of the three hydrogen structural features are common to the 6- and 11-vertex *nido*-cluster, i.e., HH and BH_2. The HH penalty is larger for the 11-vertex *nido*-cluster (25.9 kcal mol^{-1}) than that for the 6-vertex *nido*-cluster (7 kcal mol^{-1}), while the reverse is true for the BH_2 energy penalty (2.1 vs 11 kcal mol^{-1}). Although 6-vertex *nido*-clusters as well as the 11-vertex *nido*-clusters have a similar pentagonal open face, the former has three-coordinated boron atoms at the open face whereas the latter has four-coordinated boron atoms at the open face. In other words, $B^{4k}HB^{4k}HB^{4k}$ (11-vertex *nido*-cluster) is larger (25.9 kcal mol^{-1}) as compared to $B^{3k}HB^{3k}HB^{3k}$ (6-vertex *nido*-cluster, 7 or 11 kcal mol^{-1}), where superscripts show the connectivity of the boron atoms involved.

3.5.3. Mixed Energy Penalties. Out of the four mixed features (features which involve both hydrogen and carbon atoms), two, i.e., $C(BH_2)C$ and C(H), involve a hydrogen atom attached to either one or two open face boron atoms. Only $C(BH_2)C$ is part of the 6-vertex *nido*-cluster increment system. Its value for the 11-vertex *nido*-cluster (28.8 kcal mol^{-1}) is almost the same as that for the 6-vertex *nido*-cluster (25 kcal mol^{-1}).

An *endo*-terminal hydrogen attached to an open face carbon atom, symbolized as CH_2, has an energy penalty of 33.2 kcal mol^{-1} for the 11-vertex *nido*-cluster quite comparable to 30 kcal mol^{-1} for the 6-vertex *nido*-cluster.

CH−B involves a hydrogen atom bound to a carbon but tilted toward a boron atom. It behaves more like a carbon structural feature as its energy penalty varies only a little with cluster size, i.e., 27 kcal mol^{-1} for the 6-vertex *nido*-cluster versus 33.1 kcal mol^{-1} for the 11-vertex *nido*-cluster.

3.6. Comparisons of Relative Stabilities from Empirical Energy Increments (E_{inc_rel}) and from DFT Calculated Values (E_{B3LYP}) for the 11-Vertex *nido*-Boranes and Carboranes. Various known and candidate structures are ordered with the lowest energy isomer at the top for a given formula in Table 2. The most stable isomer in each case from $[B_{11}H_{14}]^-$ to $C_4B_7H_{11}$ is shown in Figure 5. Different energy penalties in a particular structure are summed up to give the E_{inc_sum}. E_{inc_rel} values are derived from E_{inc_sum} and reflect the energies relative to the most stable isomer. E_{diff} is the difference between the estimated relative energies applying the increment system, E_{inc_rel}, and DFT computed relative energies, E_{B3LYP}'s.

3.6.1. *nido*-Undecaborates, *nido*-$[B_{11}H_{14-n}]^{(1+n)-}$ ($n = 0$, 1, 2). Two possible $[B_{11}H_{14}]^-$ structures, i.e., **AA** with three bridging hydrogen atoms (μ-H, 7/8, 9/10, 7/11) and **AB** with two H-bridges and one *endo*-terminal H (μ-H, 8/9, 10/11; *endo*-H, 7) were computed. The former (**AA**) is 0.2 kcal mol^{-1} more stable than **AB**. The latter contains one structural feature, i.e., HH with a destabilizing effect of 25.9 kcal mol^{-1}. Its alternative **AB** shows two structural features, i.e., H(*endo*-H)H and BH_2 with disfavoring effects of 23.9 and 2.1 kcal mol^{-1}, respectively, giving E_{inc_sum} of 26.0 kcal mol^{-1}. E_{inc_rel} for **AB** with respect to **AA** is 0.1 kcal mol^{-1} ($E_{B3LYP} = 0.2$ kcal mol^{-1}). Attempts to optimize $[B_{11}H_{14}]^-$ with hydrogen atoms at the positions 7/8, 8/9, and 9/10 failed as the hydrogen bridges move apart from each other to give **AA**. Attempts were made to minimize the energy of two artificial geometries with twice the structural feature HH and

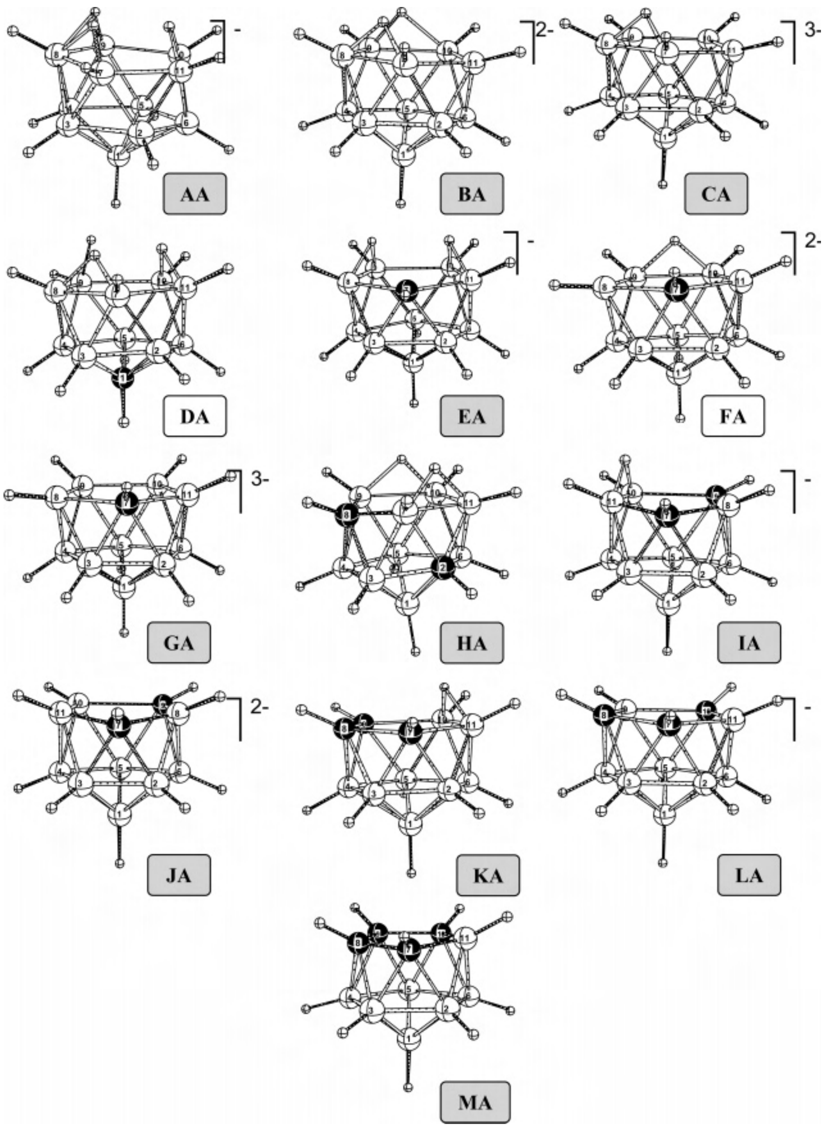

Figure 5. Most stable isomers for each molecular formula from $B_{11}H_{14}^{-}$ to $C_4B_7H_{11}$. Experimentally known structures are labeled with gray boxes.

fixed hydrogen boron bond distances to get a rough idea for the HH energy penalty. The first geometry, **AC1** (Table A in Supporting Information), with fixed hydrogen boron bridge distances taken from $CB_{10}H_{14}$ was 20.9 kcal mol^{-1} higher in energy than **AA** which is in accordance with the derived HH energy penalty. However, hydrogen boron distances fixed as in **AC2**, i.e., $H^{\mu 7/8}$−B8 and $H^{\mu 9/10}$−B9 distances which are much larger than $H^{\mu 7/8}$−B7 and $H^{\mu 9/10}$−B10 distances, give 14.9 kcal mol^{-1} relative to **AA** (Table A, Supporting Information). In other words, the more asymmetric the individual bridging hydrogen−boron distances, the more stable the cluster: In the most stable configuration, the hydrogen bridges move as far apart from each other as possible.

Two separated H-bridges in 7/8 and 9/10 positions (**BA**) result in the most stable structure (see Table 2). **BB** involves one *endo*-terminal hydrogen atom (BH_2 = 2.1 kcal mol^{-1}) and is characterized as a transition state for moving a hydrogen atom from one bridging position to the next on the open face. The latter is 2.7 kcal mol^{-1} higher in energy than **BA** by the computed results. $[B_{11}H_{13}]^{2-}$ can avoid HH by barrierless rearrangement and hence optimizes to **BA**. However, an artificial molecule, **BC** (Table A, Supporting Information), with the HH structural feature, and with fixed hydrogen boron distances, was 9.4 kcal mol^{-1} higher in energy than **BA**. For $[B_{11}H_{12}]^{3-}$, the transition state **CB** is 4.9 kcal mol^{-1} higher in energy than **CA**[19] (see Figure 3).

3.6.2. *Nido*-$[CB_{10}H_{11+n}]^{3-n}$. The presence of three extra hydrogens in *nido*-$CB_{10}H_{14}$ disfavors the open face positions for carbon placement by at least 33.2 kcal mol^{-1} (CH_2). Therefore, the carbon atom occupies the apical 5k position ($E_{inc}[C_{4k\rightarrow 5k}]$ = 28.0 kcal mol^{-1}) in the thermodynamically most stable isomer **DA**. However, the 2-isomer (**DB**) and 7-isomer (**DC**) for *nido*-$CB_{10}H_{14}$ are only slightly less stable (by 1.4 and 3.2 kcal mol^{-1}, respectively). Figure 4 shows the different structural features present in the four *nido*-$CB_{10}H_{14}$ isomers from **DA** to **DC**.

Among the four *nido*-$[CB_{10}H_{13}]^{-}$ isomers listed in Table 2, experimentally known *nido*-7-$[CB_{10}H_{13}]^{-}$ (**EA**)[1,20−22] with

---

(19) Dirk, W.; Paetzold, P.; Radacki, K. *Z. Anorg. Allg. Chem.* **2001**, *627*, 2615−2618.

the carbon atoms at the open face (a 4k position) is the most stable by 23 kcal mol^{-1}. Reduced thermodynamic stability of *nido*-1-$[CB_{10}H_{13}]^-$ (**EB**)[23] and *nido*-2-$[CB_{10}H_{13}]^-$ (**EC**) is due to a carbon atom at a 5k vertex ($C_{4k\rightarrow 5k}$). In **ED**, the carbon atom is at a least coordinated position (vertex number 7), but the presence of an *endo*-H at the carbon atom (CH_2) makes **ED** highly unfavorable.

Several structures (see Table 2) were computed for *nido*-$[CB_{10}H_{12}]^{2-}$ and *nido*-7-$[CB_{10}H_{12}]^{2-}$ (**FA**) with a hydrogen bridge between B9 and B10 found to be the most stable as it lacks any disfavoring structural feature. When hydrogen is bridged between B8 and B9 in **FB**, the structural feature C(H) gives rise to a 1.8 kcal mol^{-1} higher energy than that for **FA**. The structural features, corresponding energy penalties, $E_{\mathrm{inc\_rel}}$, and E_{B3LYP} for other *nido*-$[CB_{10}H_{12}]^{2-}$ isomers are listed in Table 2.

The experimentally known *nido*-7-$[CB_{10}H_{11}]^{3-}$ (**GA**)[12] has no high energy feature. A 5k carbon atom at apical position (**GC**) is slightly higher in energy (2.8 kcal mol^{-1}) as compared to a carbon atom at position 2 (**GB**). To both isomers **GB** and **GC**, only one energy penalty, i.e., $C_{4k\rightarrow 5k}$, applies. As mentioned above, a carbon atom at position 1 (apical position) is generally higher in energy, but only slightly, and hence was not covered by an increment of its own.

3.6.3. *nido*-$[C_2B_9H_{11+n}]^{2-n}$. Since two hydrogen atoms occupy the open face, the carbon atoms are moved to vertices of larger connectivity in the thermodynamically most stable isomer 2,8-$C_2B_9H_{13}$ (**HA**) (Figure 5). The methyl derivative of **HA** is experimentally known.[17] The isomer *nido*-1,7-$C_2B_9H_{13}$ (**HB**) has not yet been reported although thermodynamically it is more stable than two known counterparts, *nido*-2,9-$C_2B_9H_{13}$ (**HC**)[24] and *nido*-7,8-$C_2B_9H_{13}$ (**HD**).[24,25] 11-Me-*nido*-2,7-$C_2B_9H_{13}$ (11-Me-**HE**) is also experimentally known.[17]

The most stable $[C_2B_9H_{12}]^-$ isomer, i.e., *nido*-7,9-$[C_2B_9H_{12}]^-$ (**IA**),[2,24–26] has twice the structural feature C(H). *nido*-7,8-$[C_2B_9H_{12}]^-$ (**IB**)[27] has one CC and one C(H) and is 15.7 kcal mol^{-1} higher in energy than **IA**. E_{B3LYP} for **IB** (*nido*-7,8-$[C_2B_9H_{12}]^-$ with μ-H: 9/10) and **IC** (*nido*-7,8-$[C_2B_9H_{12}]^-$ with *endo*-H: 10) are very similar (see Table 2). Both **IB** and **IC** have the structural feature CC; however, structural feature C(H) in **IB** is replaced by BH_2 in **IC**. The energy penalty for C(H) (2.2 kcal mol^{-1}) is very similar to that of BH_2 (2.1 kcal mol^{-1}). A carbon atom at a 5k position in *nido*-2,9-$[C_2B_9H_{12}]^-$ (**ID**)[24] results in an increase in energy for the cluster by 25.9 kcal mol^{-1} as compared to **IA**. *nido*-7,9-$[C_2B_9H_{12}]^-$ (**IE**) with two nonadjacent carbon atoms at open face positions 7 and 9 as in **IA**, but with an *endo*-H at position number 8 (i.e. between two carbon atoms), results in a rare high energy structural feature $C(BH_2)C$ with $E_{\mathrm{inc}}[C(BH_2)C] = 28.8$ kcal mol^{-1}. A comparison of **IE** and **IA** (both differ only in the position of hydrogen atoms) shows how the position of open face hydrogen atoms affects the thermodynamic stability of clusters. *nido*-2,7-$[C_2B_9H_{12}]^-$ (**IG**) is 17.8 kcal mol^{-1} higher in energy than *nido*-2,8-$[C_2B_9H_{12}]^-$ (**IF**) mainly due to the presence of CC in the former. **IH**, **IJ**, **IK**, and **IL** are all high energy isomers due to both carbon atoms at 5k vertices (twice $C_{4k\rightarrow 5k}$). *nido*-1,7-$[C_2B_9H_{12}]^-$ (**II**) has a structural feature CH_2 along with one $C_{4k\rightarrow 5k}$ and is thermodynamically less stable than **IA** by 57.4 kcal mol^{-1}. **IJ** and **IL** also differ only in the position of the extra hydrogen atom at the open face. The latter has the structural feature twice C(H) and is 4.5 kcal mol^{-1} higher in energy than the former.

The absence of extra hydrogen atoms in $[C_2B_9H_{11}]^{2-}$ allows only two structural features, i.e., CC (16.0 kcal mol^{-1}) and $C_{4k\rightarrow 5k}$ (28.0 kcal mol^{-1}) (which quantify Williams' rules), to give the relative energy of any possible isomer. *nido*-7,9-$[C_2B_9H_{11}]^{2-}$ (**JA**) is the most stable isomer as it has no structural feature. *nido*-7,8-$[C_2B_9H_{11}]^{2-}$ (**JB**) possesses one high energy structural feature CC and is 16.3 kcal mol^{-1} higher in energy than **JA**. *nido*-2,9-$[C_2B_9H_{11}]^{2-}$ (**JC**) and *nido*-1,7-$[C_2B_9H_{11}]^{2-}$ (**JE**) both possess $C_{4k\rightarrow 5k}$, but **JE** is higher in energy than **JC** due to the apical 5k position of one carbon atom in **JE** (see section 3.3, 5k splitting). *nido*-2,8-$[C_2B_9H_{11}]^{2-}$ (**JD**) is slightly higher in energy than *nido*-2,9-$[C_2B_9H_{11}]^{2-}$ (**JC**) as the two carbon atoms are in *meta*-relationship in the former but *para*-relationship in the latter (see section 3.2.2, CC). Other structures are listed in Table 2, and their structural features and corresponding energy penalties are also given.

Known *nido*-$[C_2B_9H_{11}]^{2-}$ isomers are isolobal to cyclopentadienid, and a large number of complexes with different metal ions are known. Protonation of *nido*-7,8-$[C_2B_9H_{11}]^{2-}$ (**JB**) and *nido*-7,9-$[C_2B_9H_{11}]^{2-}$ (**JA**) formally results in *nido*-7,8-$C_2B_9H_{13}$ (**HD**) and *nido*-7,9-$C_2B_9H_{13}$ (**HG**), respectively, **HG** being higher in energy by 20.5 kcal mol^{-1} (Figure 6). The reversal of the stability order for different dicarba substitution is due to the involvement of hydrogen atoms on the open face positions in the case of *nido*-$C_2B_9H_{13}$. Carbon placement rules[5] suffice for the dicarballoid dianions, but the open face bridging hydrogens in $C_2B_9H_{13}$ over-rule the carbon placement. Our increment system successfully elaborates the behavior of carbon atoms in the presence of *endo*-hydrogen atoms on the open face.

3.6.4. *nido*-$C_3B_8H_{12}$ and *nido*-$[C_3B_8H_{11}]^-$. *nido*-7,8,9-$C_3B_8H_{12}$ (**KA**)[28] which has one hydrogen atom bridging between positions 10 and 11 (see Figure 5, Table 2) is the most stable isomer. Considering only carbon atom place-

---

(20) Onak, T. In *Boron Hydride Chemistry*; Muetterties, E. L., Ed.; Academic: New York, 1973; p 349 and references therein.

(21) Onak, T. In *Comprehensive Organometallic Chemistry*; Wilkinson, G., Stone, F. G., Abel A., E., Eds.; Pergamon: Oxford, 1982; Chapter 5.4, 411−458 and references therein.

(22) Batsanov, A. S.; Fox, M. A.; Goeta, A. E.; Howard, J. A. K.; Hughes A. K.; Malget, J. M. *J. Chem. Soc., Dalton Trans.* **2002**, 2624−2631.

(23) Beer, D. C.; Burke, A. R.; Engelmann, T. R.; Storhoff, B. N.; Todd. L. J. *J. Chem. Soc., Chem. Commun.* **1971**, *24*, 1611−1612.

(24) Fox, M. A.; Goeta, A. E.; Hughes, A. K.; Johnson, A. L. *J. Chem. Soc., Dalton Trans.* **2002**, *10*, 2132−2141.

(25) (a) Wiersboeck, R. A.; Hawthorne, M. F. *J. Am. Chem. Soc.* **1964**, *86*, 1642−1643. (b) Hawthorne, M. F.; Young, D. C.; Garett., P. M.; Owen, D. A.; Schwerin, S. G.; Tebbe, F. N.; Wegner, P. A. *J. Am. Chem. Soc.* **1968**, *90*, 862−868.

(26) Leites, L. A.; Bukalov, S. S.; Vinogradova, L. I.; Kalinin, V. I.; Kobel'kova, N. I.; Zakharian, L. I. *Izv. Akad. Nauk SSSR, Ser. Khim.* **1984**, 954.

(27) Fox, M. A.; Goeta, A. E.; Howard, J. A. K.; Hughes, A. K.; Johnson, A. L.; Keen, D. A.; Wade, K.; Wilson, C. C. *Inorg. Chem.* **2001**, *40*, 173−175.

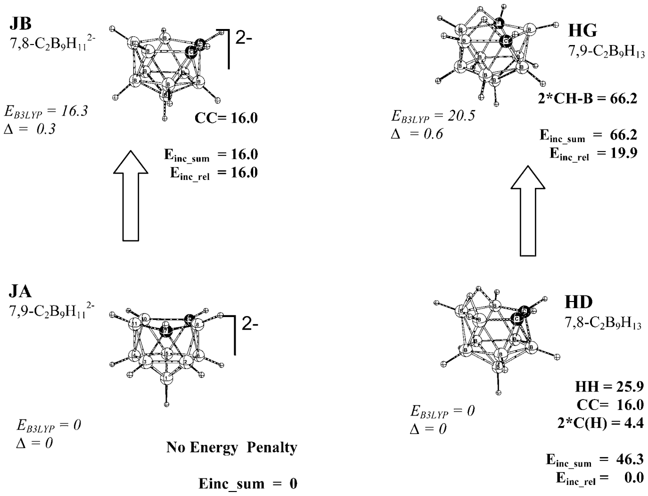

Figure 6. Comparison of 7,8- and 7,9- isomers for *nido*-$C_2B_9H_{11}^{2-}$ and *nido*-$C_2B_9H_{13}$.

ment,[5] 7,8,10-$C_3B_8H_{12}$ (**KB**) should be the best, but the presence of one extra hydrogen atom at the open face results in less stability than **KA**.

nido-7,8,10-$[C_3B_8H_{11}]^-$ (**LA**)[28] has the structural feature CC once, and *nido*-7,8,9-$[C_3B_8H_{11}]^-$ (**LB**)[28] has it twice. Consequently, **LA** (Figure 5, Table 2) is more stable than **LB** by 18.5 kcal mol^{-1}.

3.6.5. *nido*-$C_4B_7H_{11}$. The ab initio/IGLO/NMR method has been applied to establish the structures of the three isomers of *nido*-$C_4B_7H_{11}$ to be *nido*-7,8,9,10-$C_4B_7H_{11}$ (**MA**)[29,30] (Figure 5), *nido*-1,7,8,10-$C_4B_7H_{11}$ (**MB**)[30] (rather than *nido*-1,2,8,10-$C_4B_7H_{11}$),[31] and *nido*-2,7,9,10-$C_4B_7H_{11}$ (**MC**)[29] (rather than *nido*-2,7,8,11-$C_4B_7H_{11}$).[30] Three structures, i.e., *nido*-7,8,9,10-$C_4B_7H_{11}$ (**MA**) (Figure 5), *nido*-1,7,8,10-$C_4B_7H_{11}$ (**MB**), and *nido*-2,7,9,10-$C_4B_7H_{11}$ (**MC**), are included here. Reversal of stability order between E_{B3LYP} and E_{inc_rel} is observed for **MA** and **MB**. The most stable structure **MA** (Figure 5) has a unique feature, i.e., four of its five peripheral vertices are occupied by carbon atoms giving rise to three consecutive adjacent carbon relationships, a structural feature which is not observed in any other known carborane isomer. A large number of carbon atoms in *nido*-undecaborane isomers causes a significant distortion of the cluster; while the increment approach still works, the assumption of additivity is less valid. The reported[30] MP2/6-31G*//6-31G*+ZPE and 6-31G*//6-31G*+ZPE relative energies when compared with the values estimated from increments reported here deviate by slightly more than 5 kcal mol^{-1}.

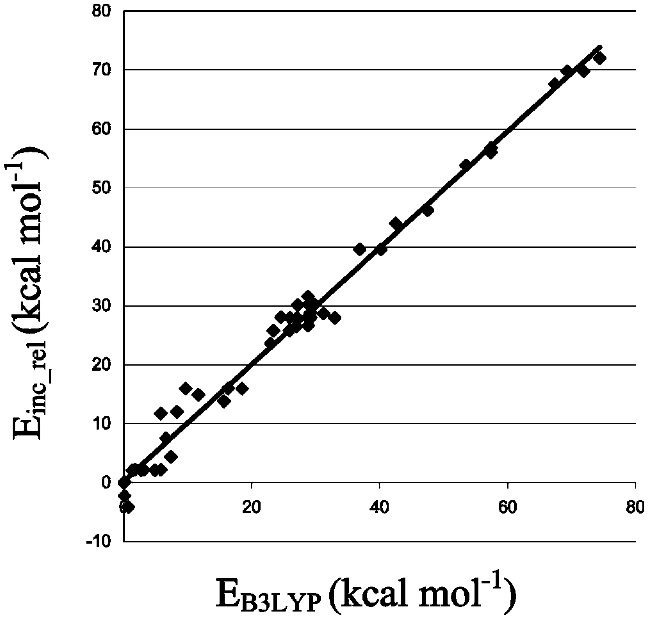

Figure 7. Structural increments accurately reproduce the relative stabilities of 11-vertex *nido*-(car)boranes computed by DFT methods.

Figure 7 indicates how accurately nine structural features can reproduce the relative stability order produced by DFT calculations. Considering 61 examples from $[B_{11}H_{14}]^-$ to $C_4B_7H_{11}$, the difference between the E_{inc_rel} and E_{B3LYP} is 2 kcal mol^{-1} or less in 42 cases. In all the cases from $[B_{11}H_{14}]^-$ to $C_4B_7H_{11}$, the stability order as derived from the presented increment system is the same as the computed one except in five cases: **DD** (7-$CB_{10}H_{14}$) with E_{inc_rel} and E_{B3LYP} of

---

(28) Holub, J.; Štíbr, B.; Hnyk, D.; Fusek, J.; Císařová, I.; Teixidor, F.; Viñas, C.; Plzák, Z.; Schleyer, P. v. R. *J. Am. Chem. Soc.* **1997**, *119*, 7750−7759.

(29) Štíbr, B.; Jelínek, T.; Drdáková, E.; Heřmánek, S.; Plešek, J. *Polyhedron* **1988**, *8*, 669−670.

(30) Bausch, J. W.; Rizzo, R. C.; Sneddon, L. G.; Wille, A. E.; Williams, R. E. *Inorg. Chem.* **1996**, *35*, 131−135.

(31) Astheimer, R. J.; Sneddon, L. G. *Inorg. Chem.* **1983**, *22*, 1928−1934.

(32) (a) Volkov, O.; Radacki, K.; Paetzold, P.; Zheng, X. *Z. Anorg. Allg. Chem.* **2001**, *627*, 1185−1191 and references therein. (b) Volkov, O.; Radacki, K.; Thomas, R. Ll.; Rath, N. P.; Barton, L. *J. Organomet. Chem.*, to be published.

(33) Afiandilian, V. D.; Miller, H. C.; Parshall, G. W.; Muetterties, E. L. *Inorg. Chem.* **1962**, *1*, 734−737.

(34) Hosmane, N. S.; Wermer, J. R.; Hong, Z.; Getman, T. D.; Shore, S. G. *Inorg. Chem.* **1987**, *26*, 3638−3639.

(35) Getman, T. D.; Krause, J. A.; Shore, S. G. *Inorg. Chem.* **1988**, *27*, 2398−2399.

(36) McGrath, T. D.; Welch, A. J. *Acta Crystallogr.* **1997**, *C53*, 229−231.

(37) Maitre, P.; Eisenstein, O.; Michos, J. D.; Xiao-Liang L.; Siedle, A. R.; Wisnieski, L.; Zilm, K. W.; Crabtree, R. H. *J. Am. Chem. Soc.* **1993**, *115*, 7747−7751.

(38) Volkov, O.; Paetzold, P. *J. Organomet. Chem.* **2003**, *680*, 301−311.

(39) Getman, T. D. Ohio State University, Columbus, OH, 1988. Available from University Microfilms Int., Order No. DA8812249, 152 pp. *Diss. Abstr. Int. B* **1988**, *49*, 1164.

(40) Fritchie, C. J. *Inorg. Chem.* **1967**, *6*, 1199−1203.

(41) Harmon, K. M. *J. Mol. Struct.* **2002**, *612*, 65−68.

(42) Whitaker, C. R.; Romerosa, A.; Teixidor, F.; Rius, J. *Acta Crystallogr.* **1995**, *C51*, 188−190.

(43) Plešek, J.; Heřmánek, S. *Chem. Ind.* **1973**, *8*, 381−382.

(44) Mackie, I. D.; Robertson, H. E.; Rankin, D. W. H.; Fox, M. A.; Malget, J. M. *Inorg. Chem.* **2004**, *43*, 5387−5392.

(45) Davidson, M. G.; Fox, M. A.; Hibbert, T. G.; Howard, J. A. K.; MacKinnon, A.; Neretin, I. S.; Wade, K. *Chem. Commun.* **1999**, 1649−1650.

(46) Buchanan, J.; Hamilton, E. J. M.; Reed, D.; Welch, A. *J. Chem. Soc., Dalton Trans.* **1990**, 677−680.

(47) Busby, D. C.; Hawthorne, M. F. *Inorg. Chem.* **1982**, *21*, 4101−4103.

(48) Knyazev, S. P.; Brattsev, V. A.; Stanko, V. I. Inst. Biofiz., Moscow, USSR. *Dokl. Akad. Nauk* **1977**, *234*, 837−840.

(49) Green, M.; Spencer, J. L.; Stone, F. G. A.; Welch, A. J. *J. Chem. Soc., Chem. Commun.* **1974**, *14*, 571−572.

(50) Hawthorne, M. F.; Young, D. C.; Andrews, T. D.; Howe, D. V.; Pilling, R. L.; Pitts, A. D.; Reintjes, M.; Warren, L. F.; Wegner, P. A. *J. Am. Chem. Soc.* **1968**, *90*, 879−896.

(51) Greenwood, N. N.; Earnshaw, A. *Chemistry of the Elements*, 1st ed.; Pergamon Press: Oxford, 1984; p 209.

(52) Zalkin, A.; Templeton, D. H.; Hopkins, T. E. *J. Am. Chem. Soc.* **1965**, *87*, 3988−3990.

(53) Kaloustian, M. K.; Wiersema, R. J.; Hawthorne, M. F. *J. Am. Chem. Soc.* **1971**, *93*, 4912−4913.

7.5 and 6.6 kcal mol^{-1}, respectively, and **DE** (2-$CB_{10}H_{14}$) with E_{inc_rel} and E_{B3LYP} of 4.4 and 7.4 kcal mol^{-1}, respectively. E_{inc_rel} of **HB** (1,7-$C_2B_9H_{13}$) is −2.2 kcal mol^{-1}, but **HA** (2,8-$C_2B_9H_{13}$) is 0.6 kcal mol^{-1} more stable than **HB** from the E_{B3LYP} results. E_{inc_rel} values for **IB** and **IC** (13.8 and 13.6 kcal mol^{-1}) are reverse to E_{B3LYP} values (15.7 and 15.9 kcal mol^{-1}). Reversal of the stability order is also observed in $C_4B_7H_{11}$: The increment system predicts 1,7,8,10-$C_4B_7H_{11}$ (**MB**) to be more stable by a value of 4.0 kcal mol^{-1}, but 7,8,9,10-$C_4B_7H_{11}$ (**MA**) is more stable by 0.7 kcal mol^{-1} according to the DFT computed results. The stability order is also reversed for **HG** and **HH**. In three of the five cases, where the stability order is reversed, i.e., **HA** and **HB**, **HG** and **HH**, as well as **MA** and **MB**, the correct order can be recovered by considering a 5k apical carbon atom to be slightly higher in energy than at positions 2−6. **DD** is the only possible 11-vertex *nido*-cluster that contains a CH_2 group between two hydrogen bridges. For this structural feature, an energy penalty of ∼20.0 kcal mol^{-1} can be derived. However, it cannot be proven to be generally valid as only one example is possible. Furthermore, the value is close to the H(*endo*-H)H energy penalty (23.9 kcal mol^{-1}), where the *endo*-H is attached to a boron rather than a carbon atom, and hence, both were treated together as H(XH_2)H ($X = B, C$).

Two unknown 11-vertex *nido*-dicarbaboranes, i.e., 1,7-$C_2B_9H_{13}$ and 2,8-$[C_2B_9H_{12}]^-$, are thermodynamically more stable than known isomers (see Table 2). 7,9-$[C_2B_9H_{12}]^-$ with an *endo*-H is also thermodynamically more stable than known 2,7-$[C_2B_9H_{12}]^-$, but its counterpart **IA** is the most stable $[C_2B_9H_{12}]^-$ isomer. This increment system is not limited to the typical 61 isomers it was derived from, but it can be applied to many more 11-vertex *nido*-carboranes structures. A similar kind of increment system might be derived for heteroatoms other than carbon.

4. Conclusions

An increment system was established for the 11-vertex *nido*-boranes and carboranes. Nine architectural features are sufficient to accurately estimate the relative stabilities of 61 and probably more 11-vertex *nido*-isomers from $[B_{11}H_{14}]^-$ to $C_4B_7H_{11}$ (see Figure 7). The energy penalties assigned can be divided into three main groups, carbon structural features which do not change much between the 6- and the 11-vertex *nido*-clusters and hydrogen structural features which depend strongly on the connectivity (k) of the boron atoms to which they are attached. Mixed structural features in which an *endo*-hydrogen is attached to a carbon atom behave more like carbon structural features, and those features in which an *endo*-hydrogen is attached to boron atoms behave like hydrogen structural features. Applying our increment system, two carboranes were identified which are not yet known experimentally, but which are thermodynamically more stable than known isomers and hence should be synthesizable.

Acknowledgment. Financial support by DFG (Deutsche Forschungsgemeinschaft) is gratefully acknowledged.

Supporting Information Available: Results of computation on constrained $[B_{11}H_{14}]^-$ geometries (Table A) and Cartesian coordinates and absolute energies from B3LYP/6-31G* optimizations of $[B_{11}H_{14}]^-$ to $C_4B_7H_{11}$ structures discussed in sections 3.6.1−3.6.11, Tables 2 and 3, and Figures 3−6. This material is available free of charge via the Internet at http://pubs.acs.org.

IC049184Z